INTERNATIONAL JOURNAL OF CLIMATOLOGY
Int. J. Climatol. **29**: 983–992 (2009)
Published online 3 June 2008 in Wiley InterScience
(www.interscience.wiley.com) DOI: 10.1002/joc.1720

RMetS
Royal Meteorological Society

Impact of African orography and the Indian summer monsoon on the low-level Somali jet

Arindam Chakraborty,[a]* Ravi S. Nanjundiah,[b] and J. Srinivasan[b]
[a] *Department of Meteorology, Florida State University, Tallahassee, FL 32306, USA*
[b] *Centre for Atmospheric and Oceanic Sciences, Indian Institute of Science, Bangalore 560012, India*

ABSTRACT: The low-level jet (LLJ) over the Indian region, which is most prominent during the monsoon (June–September) season, has been studied with a general circulation model (GCM). The role of African orography in modulating this jet is the focus of this article. The presence of African orography intensifies the cross-equatorial flow. Contrary to previous modelling studies we find that cross-equatorial flow occurs even in the absence of African orography, though this flow is much weaker even when the Indian monsoon rainfall is high. However, the location of the meridional jet near the equator in the Somali region is linked to the Indian monsoon rainfall rather than to the land–sea contrast over Somalia. Also, the presence of African orography, and not the strength of the Indian monsoon, controls the vertical extent of the equatorial meridional wind.

In an aqua-planet simulation, the cross-equatorial flow occurs about 30° to the west of the rainfall maximum. Thus, the longitudinal location of the equatorial Somali jet depends upon the occurrence of monsoon heating, but the vertical structure of the jet is on account of the western boundary current in the atmosphere due to the East African highlands under the influence of monsoonal heat source. Copyright © 2008 Royal Meteorological Society

KEY WORDS Somali jet; African orography; Indian summer monsoon; general circulation model

Received 25 October 2007; Revised 9 April 2008; Accepted 14 April 2008

1. Introduction

The summer monsoon over the Indian region is associated with a low-level jet (LLJ). The jet has maximum winds at about 850 hPa and is most prominent during the June–September season. Joseph and Raman (1966) first identified the existence of the jet over the Indian peninsula. Findlater (1969a,b) showed that its origin was in the trade-wind easterlies over the southern Indian Ocean, and crossed the equator along a narrow longitudinal belt over the Somalia coast near the East African mountains followed by an eastward turning into the Indian region where it is predominantly a westerly jet.

The impact of the East African mountains on the LLJ was first studied by Krishnamurti *et al.* (1976). They used a one-level primitive equation model that incorporated detailed orographic features of the east African mountains. Their study highlighted the importance of the East African mountains, land–sea contrast and beta effect on the simulation of the LLJ. The baroclincity in the boundary layer and its effect on the LLJ was further studied by Krishnamurti and Wong (1979) and Krishnamurti *et al.* (1983).

Hoskins and Rodwell (1995) and Rodwell and Hoskins (1995) studied the LLJ with a primitive equation model with specified zonal flow, orography and diabatic heating. They showed that the presence of East African orography, and land–sea contrast due to orography played an important role for the intensification of the cross-equatorial flow. Sashegyi and Geisler (1987) studied the impact of diabatic heating on the strength of the jet in a linear model. In the absence of a western boundary, no cross-equatorial flow developed. Upon prescription of a western boundary, a strong northward flow appeared in their simulations and they concluded that the strong meridional jet seen near the African coast is a western boundary current. Mawson and Cullen (1992) studied the impact of diabatic heating on the Somali jet with a linear primitive equation model and found similar cross-equatorial fluxes. Most of these studies on various aspects of the LLJ have been conducted with linear models.

Chakraborty *et al.* (2002) used a general circulation model (GCM) to study the role of African orography on the Indian monsoon. They found that in their simulations, the strength of the Indian monsoon increased when the East African mountains were removed. They showed that there existed a positive non-linear feedback loop between the Indian monsoon rainfall and the strength of the jet. Joseph and Sijikumar (2004) have studied the intra-seasonal variability of LLJ using the NCEP/NCAR (National Center for Environmental Prediction/National Center for Atmospheric Research) re-analysis datasets. They found that the jet axis is northward of its seasonal mean position during active spells (periods of high

* Correspondence to: Arindam Chakraborty, Department of Meteorology, Florida State University, Tallahassee, FL 32306, USA.
E-mail: arindam@met.fsu.edu

rainfall over the Indian region) and southward (with the jet avoiding the Indian sub-continent) during periods of low Indian rainfall. Slingo *et al*. (2005), in a study using an atmospheric general circulation model (AGCM) and European Centre for Medium-Range Weather Forecasts 40-year Re-analysis (ERA40) suggest that the role of the East African highlands is to intensify the hydrological cycle over the Indian region and to focus the monsoonal winds along the coast.

The magnitude of the LLJ is linked non-linearly to the rainfall over the Bay of Bengal region. Srinivasan and Nanjundiah (2002) have shown that, on synoptic time-scales, the speed of the jet over the Arabian Sea lags latent heating over the Bay of Bengal by about 3 days. Hence, it is necessary to study the impact of the East African mountains and the latent heating in the Bay of Bengal on the LLJ with a non-linear model such as an AGCM. Kitoh (2004), investigating the impacts of orography on monsoon with an atmosphere–ocean coupled and a non-coupled model, showed that a large number of features obtained from the coupled model simulations were also present in the results from the corresponding AGCM. In this article we address the following issues with an AGCM:

1. The factors that govern the strength of the LLJ.
2. The relative roles of East African orography and latent heating on the LLJ.

2. The model details and numerical experiments

The global spectral AGCM used in the present study is the NCEP model (Sela, 1982, 1988). It is a spectral model with triangular truncation at 80 waves (T80), which gives an approximate horizontal grid size of 140 km $\times$ 140 km near the Equator. The model has 18 levels in the vertical. Surface fluxes are calculated based on vertical stability (using the bulk Richardson number and the Monin–Obhukov theory) following the method of Pan and Mahrt (1986). The model's shortwave radiation scheme is based on Lacis and Hansen (1974), and the longwave radiation scheme is based on Fels and Schwarzkopf (1981). Cumulus convection is parameterized using the Simplified Arakawa Schubert (SAS) after Grell (1993), and incorporates downdrafts and re-evaporation of precipitation.

The control simulation of our model used mean orography all over the globe. To understand the role of African orography, we conducted an experiment in which orography from the entire African continent was removed (referred to as *noAfOrog* in this article). We also conducted simulations in which mountains were retained only over Africa while removing them from across the rest of the planet (referred to as *prAfOrog* in this article). In a third perturbed experiment, mountains over the entire globe were removed (referred to as *noGlOrog* in this article). In addition to these simulations, we have performed an aqua-planet simulation where all land points were replaced by ocean in the model. In this simulation, a circular region of high sea surface temperature (SST) (302 K) was centered at 90 °E and reduced linearly to 288 K within 10°. This region mimics the observed monsoonal heat source at the head of the Bay of Bengal. Diurnal and seasonal variations of solar forcing similar to that prescribed in the control were included in the aqua-planet simulations. Table I describes the simulations used in this article and their nomenclature.

All experiments (except the aqua-planet simulation which had one member corresponding to 1 March 1998) were based on an ensemble of five members starting with different initial conditions corresponding to 1–5 March 1998. Choice of the year for our experiments was rather arbitrary. We have conducted a few experiments during other years as well, and essential features of the results remained unchanged and do not depend upon the year. The initial states for the model were taken from NCEP/NCAR re-analysis dataset. Monthly mean SST for 1998 were prescribed from Reynolds and Smith (1994). All results presented in this article are based on the mean over the five ensemble members of a simulation (except the aqua-planet simulation which was based on one member) conducted for the year 1998.

3. Structure of the low-level jet: observations and control simulations

The observed structure of the LLJ over the equatorial Indian Ocean and Arabian Sea during the boreal summer season of 1998 from ERA40 datasets (Uppala *et al*., 2005) is shown in Figure 1(a). The LLJ can be divided into four distinct regions. Moving from east to west we can classify them as

1. A zonal westerly jet with a maximum around 10°N over the Indian region extending between 55 °E and 90 °E;

Table I. The experiments performed and the nomenclatures used in this article.

Description	Nomenclature
Mean orography all over the globe	Control
Mountains removed from the entire African continent	noAfOrog
Mountains retained only over the African continent and removed from the rest of the globe	prAfOrog
Mountains removed from all across the globe	noGlOrog
Aqua-planet simulation with maximum SST of 302 K centered at 90 °E, 20 °N	AP302

DOI: 10.1002/joc

2. Southwesterly flow between 55 °E and the coast of Africa to the north of the Equator;
3. Meridional jet around the Equator near the east coast of Africa; and
4. Southeasterly flow south of the Equator.

The jet begins to develop in May and is strongest during the month of July when the strength of the Indian summer monsoon is highest. Figure 1(a) also shows that the cross-equatorial flow was much less over the regions east of 65 °E and west of 40 °E as compared to the East African coast (40°–60 °E). The major goal of this article is to investigate the reasons behind the location, strength and the vertical structure of this jet using a GCM that allows realistic feedback between different atmospheric processes. A comparison of Figure 1(a) and (b) shows that the maximum wind speed near 50 °E, 10°N was realistic in the model's control simulation. The cross-equatorial flow, similar to that in the observations, was confined to near the East African mountains along the Somalia coast. The wind speed south of the Equator and over the Bay of Bengal and Indian peninsular were also well captured by the model. However, it can be noted that the model winds over the northern parts of the Indian Ocean are too zonal, and the model does not capture the curvature in the wind field near the southern tip of India. The westerlies over central and north India are weak in the model compared to the ERA40 data. The overall agreement of the model with the ERA40 data sets suggests that this model can be used to perform perturbed simulations to understand the characteristics of this LLJ.

The vertical structures of the LLJ along 60 °E and the zonal cross-section at the Equator from observations and control simulation of the model during July 1998 are shown in Figure 2. In the observations (Figure 2(a)) below the 800 hPa level, the zonal wind is westerly, north of the Equator, and easterly in the south. The peak of the westerly flow in the Northern Hemisphere was located at around 12°N latitude and 850 hPa pressure level. The value of this peak zonal flow exceeded 18 m s^{-1}. The

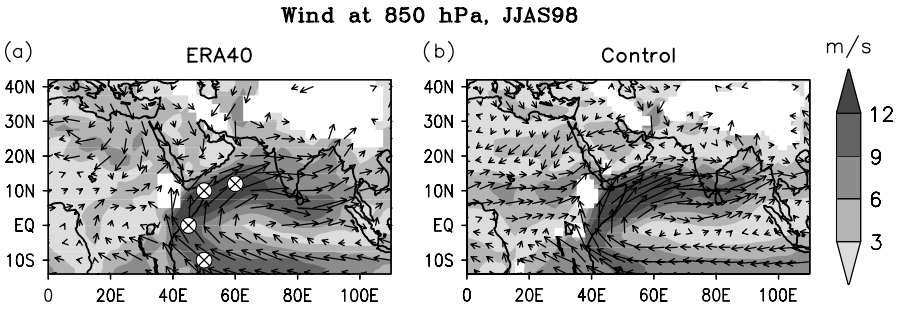

Figure 1. Horizontal wind speed (shaded) and direction (vector) during the summer season (June-September) of 1998 from (a) observation (ERA40) and (b) control simulation of the model at 850 hPa. Regions where the height of this pressure level was less than the orographic height were left with no data. The crossed circles in panel (a) indicate locations where vertical profiles of horizontal winds were studied (Figure 3).

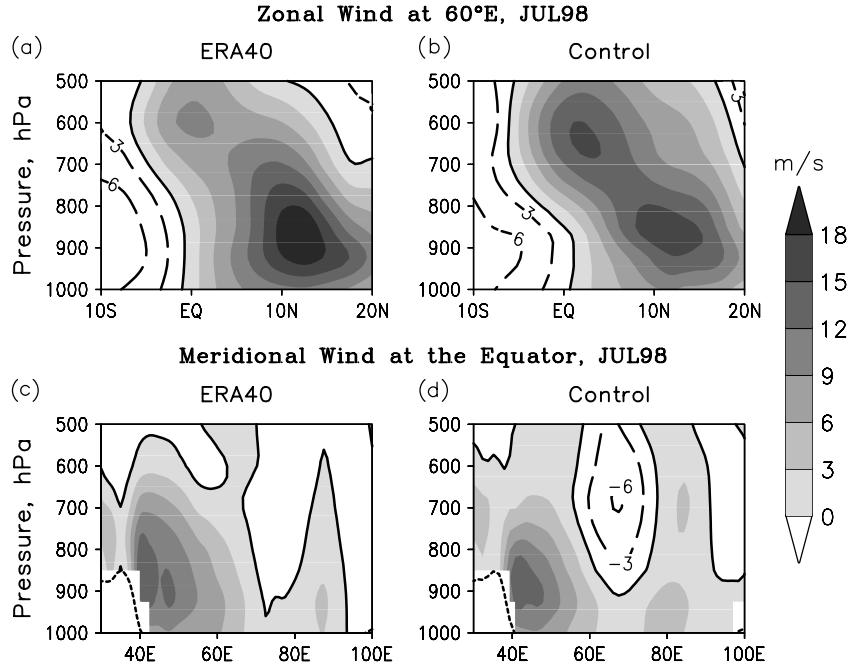

Figure 2. Vertical structure of the LLJ during July 1998, from observations (ERA40) and control simulation. (a) and (b): Zonal wind at 60 °E; (c) and (d): Meridional wind at the equator.

DOI: 10.1002/joc

control simulation (Figure 2(b)) was able to capture this location of the maxima both in terms of latitude and height. However, the maximum value in the model was about 3 m s^{-1} less compared to that in the observations. Above 800 hPa, the westerly wind extends up to 5 °S (Figure 2(a)). A secondary westerly wind maximum is noticed near the Equator at around 600 hPa level in the observed datasets. This indicates a north–south tilt of the westerly jet in the vertical. The control simulation of the model realistically captures this north–south tilt in the vertical (Figure 2(b)).

The vertical structure of the meridional wind at the Equator is shown in Figure 2(c) and (d) Also shown in these panels are the East African mountains (dashed lines). Major cross-equatorial flow occurred between 40° and 65 °E and below 600 hPa pressure level. These figures also show that the cross-equatorial flow was maximum at 850 hPa just off the East African mountains. Note that maximum wind speed of the cross-equatorial flow (Figure 2(c)) is weaker by about 6 m s^{-1} compared to the maximum westerly wind speed at 60 °E (Figure 2(a)). The cross-equatorial flow was well simulated by the control simulation of the model (Figure 2(d)). However, the return flow towards the Southern Hemisphere between 60° and 80 °E was stronger in the control simulation when compared to the observations. However, we found that the return flow in NCEP Re-analysis is stronger when compared to ERA40, and hence, this feature of the model may not be unrealistic.

In Figure 3, we have shown the profiles of zonal and meridional winds at four locations (indicated by crossed circles in Figure 1(a)) along the axis of the jet during July 1998. South of the Equator, at 50 °E, 10 °S, the zonal wind is easterly with its peak between 925 and 850 hPa levels (Figure 3(a)). Meridional wind at the same location (Figure 3(e)) is southerly, which indicates a southeasterly flow. At the Equator near the East African mountains (45 °E), meridional wind from ERA40 datasets is 6–8 times stronger than the zonal wind at the same location. This strong cross-equatorial jet is confined mainly below the 700 hPa level. The control simulations of the model could realistically capture this feature of the meridional flow in the lower troposphere (Figure 3(f)) although the zonal wind was stronger in the model (Figure 3(b)). After crossing the Equator, the horizontal winds become southwesterly with a stronger zonal component at 50 °E, 10°N (Figure 3(c), (g)). It is to be noted that the peak of the zonal wind at this location was between 700 and 850 hPa levels, whereas the peak of the meridional winds was at 925 hPa level. The control experiment was able to simulate this vertical structure quite well. Further eastward over the Arabian Sea at 60 °E, 12 °N, the zonal wind had a larger component as compared to its meridional counterpart (Figure 3(d), (h)). The peak of the zonal wind was 850 hPa, and that of the meridional wind was 925 hPa at this location. These features are also well simulated by the control experiment.

From the above analysis we find that the model is capable of realistically producing the low-level monsoon jet. In the next section, we discuss the impact of the East African highlands on the LLJ.

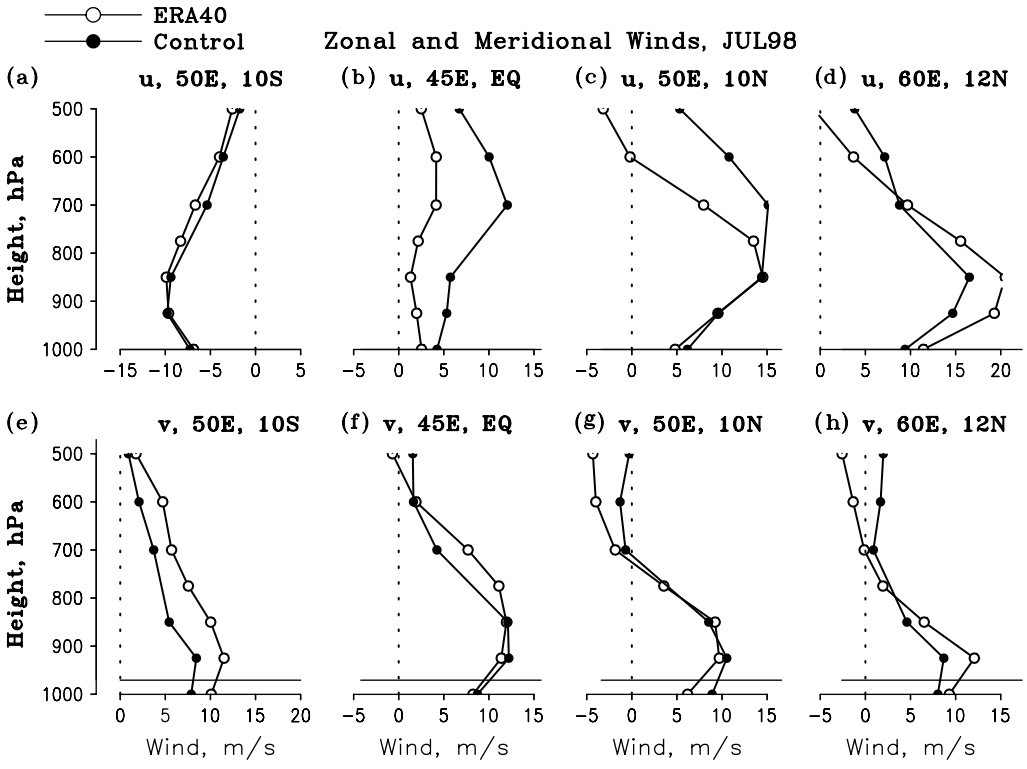

Figure 3. Vertical profile of (a–d) zonal and (e–h) meridional winds at four locations along the axis of the LLJ from observations (ERA40) and model control simulation during July 1998. These locations are marked as crossed circles in Figure 1(a).

DOI: 10.1002/joc

4. Impact of African orography on the low-level jet

Three sets of experiments were performed to understand the role of the mountains of Africa on the LLJ. In the first experiment, orography from the entire African continent alone was removed (*noAfOrog*). The design of this experiment differs with control only in the absence of African orography. In the second experiment, orography was included only over the African continent but was removed from all other parts of the world (*prAfOrog*). This experiment can be viewed as the inverse of *noAfOrog*. The third experiment did not include any orography over the globe (*noGlOrog*). Therefore, this experiment differs from *prAfOrog* only in the absence of African orography. Chakraborty *et al*. (2002) and Chakraborty *et al*. (2006) have shown that in the absence of African orography, the Indian summer monsoon rainfall increases but there is no significant impact on the date of onset of the Indian summer monsoon. Therefore, it will be interesting to see from these four experiments of the GCM, how East African orography affects the LLJ over the western Arabian Sea near the Equator.

Figure 4 (a–d) show the vertical structure of meridional wind at the Equator from control, *noAfOrog, prAfOrog* and *noGlOrog* simulations, respectively, during July. The cross-equatorial jet is noticed at around 40°–45 °E irrespective of whether East African mountains are present or absent in the model. However, upon inclusion of East African orography the jet was stronger and the location of the maximum wind was at a higher level (above sea level).

Figure 5 (a–d) show the spatial distribution of precipitation during July from control, *noAfOrog, prAfOrog* and *noGlOrog* simulations respectively. There are some differences in the location and magnitude of precipitation maxima obtained in the control simulation when compared to observations (not shown). For example, the model is too dry over northern India, near the foothills of the Himalayas, and too wet over the central and southern Indian peninsula. The model also overestimates the precipitation maximum over the Arabian Sea. The high precipitation over the northern Bay of Bengal is shifted a few degrees southward in the model. However, the model control simulation captures the overall characteristics of the South Asian monsoon rainfall. The ensemble mean precipitation averaged over the Indian region during June–September is very close to the observed value (Chakraborty *et al*., 2006). The seasonal variation of precipitation is also well simulated by the model.

It can be seen from Figure 5 that two distinct classes of precipitation patterns exist over the Arabian Sea in these four experiments. When Himalayan orography is present (control and *noAfOrog*) the location of precipitation maximum is around 15°–20 °N. This maximum shifts to around 10°N without Himalayan orography (*prAfOrog* and *noGlOrog*). However, the location of maximum precipitation over the Bay of Bengal appears to be independent of the presence of the Himalayan and African mountains. The amount of precipitation was higher over the Bay of Bengal in the absence of African orography when other conditions remained unchanged (compare *noAfOrog* with control, and *noGlOrog* with *prAfOrog*). Figure 5 also shows that precipitation over eastern Africa and the Somalia coast was almost absent when African orography was removed. This is to be expected since there was no orographic rainfall in these regions. The seasonal mean precipitation over the Indian region increased by 28% in the *noAfOrog* simulation as compared to control. This could be due to changes in surface conditions in this experiment. Without African orography, the surface over the African continent is smooth and convection is weak. At the same time, since precipitation was high over the Bay of Bengal,

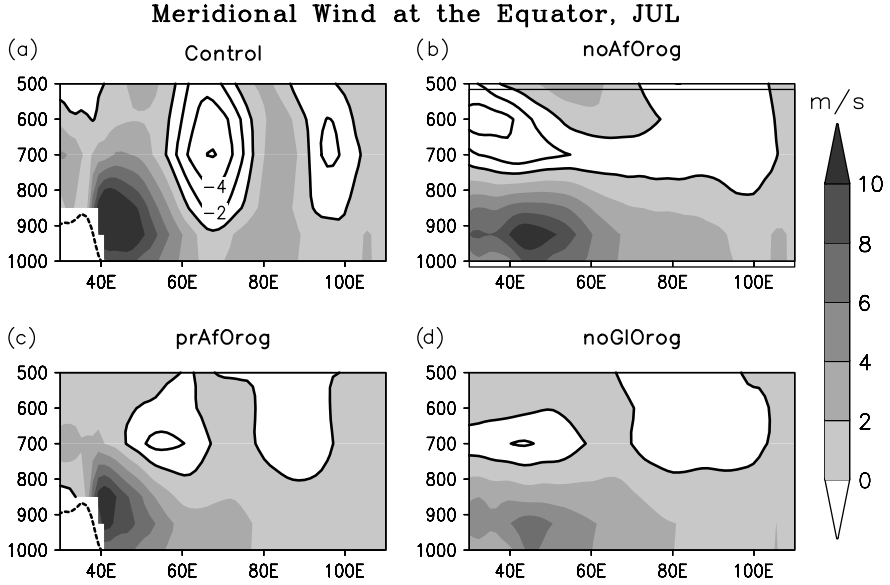

Figure 4. Meridional wind at the equator during July from (a) control (all orography present), (b) *noAfOrog* (all but African orography present), (c) *prAfOrog* (all but African orography absent), and (d) *noGlOrog* simulations (all orography absent). The orographic height for control and *prAfOrog* is shown by dotted lines in the respective panels.

DOI: 10.1002/joc

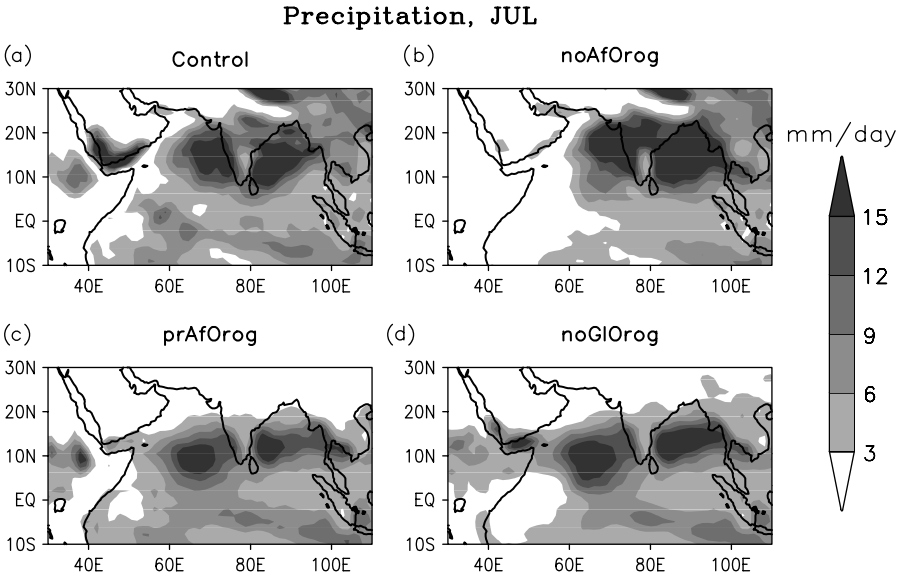

Figure 5. Precipitation during July from (a) control (all orography present), (b) *noAfOrog* (all but African orography present), (c) *prAfOrog* (all but African orography absent), and (d) *noGlOrog* simulations (all orography absent).

the wind over the Somalia coast was also high. This draws more moisture towards the Indian sub-continent. However, the oceanic condition remained unchanged, and convective systems formed over oceans in all the perturbed simulations. Due to this reason, two regions of maximum precipitation are seen over the Arabian Sea and Bay of Bengal irrespective of the presence of the Himalayan or African mountains. The location of maximum precipitation over the South Asian monsoon region drives the cross-equatorial jet near the Somalia coast during this month (Figure 4).

The most striking feature about the equatorial meridional winds is the concentration of isotachs near the African coast in the control simulation. The structure appears to be more diffused, and meridional winds are weaker in the *noAfOrog* and *noGlOrog* simulations. However, it is noteworthy that while the region of southerly winds is broader in the *noAfOrog* simulation and there is no concentration of isotachs near the African coast, the wind maximum is still centered at 45 °E. This position appears to be independent of the presence of African orography. We also find that the northward flow in the meridional jet at the Equator is deeper in observations and in the control simulation with southerly winds reaching up to 500 hPa. In contrast, the southerly winds reach only up to 750 hPa in the *noAfOrog* and *noGlOrog* simulations. The depth of the equatorial meridional jet is not related to the strength of the Indian monsoon rainfall as the rainfall is highest in *noAfOrog* and lowest in *noGlOrog* (Chakraborty *et al*., 2006), but the depth of the jet in both the simulations is the same. Under control simulations in which the Indian monsoon rainfall is lower than in *noAfOrog*, the equatorial meridional jet is deeper. Thus, it is the presence of African orography and not the strength of the Indian monsoon that decides the depth of the equatorial meridional jet. In the presence of African orography, the southeasterly flow south of the Equator hits the East African mountain barrier and crosses the equator essentially confined to a narrow region between 40° and 60 °E. The cross-equatorial mass flux through this narrow region essentially increases the depth of the LLJ in these simulations.

Figure 6 (a–d) show the zonal wind at 60 °E from control, *noAfOrog, prAfOrog* and *noGlOrog* simulations. Note that the vertical structure of zonal wind is similar for control and *noAfOrog* simulations. However, the strength of the zonal wind was much higher when orography was removed from the African continent (compare control vis-à-vis *noAfOrog*). The same is true for *prAfOrog* and *noGlOrog* simulations. The zonal wind over the Arabian Sea increased when orography was removed from over the African continent while going from *prAfOrog* simulation to *noGlOrog* simulation. The strengthening of the horizontal wind north of the Equator and large change in cross-equatorial flow (Figure 4) without African mountains was similar to that obtained by Park and Hong (2004) using a regional model. However, our results show stronger easterlies south of the Equator those were absent in the regional model study of Park and Hong (2004).

Figure 7 (a–d) show the horizontal wind at 850 hPa during July from control, *noAfOrog, prAfOrog* and *noGlOrog* simulations. In this figure, we have also shown the approximate axis of the LLJ at this pressure level as a dashed line. The axis of the LLJ was determined from local maxima (within a $2^\circ \times 2^\circ$ box in longitude–latitude) of the wind fields of the respective simulations. We find that there is an increase in zonal winds over most of the Arabian Sea and the Indian sub-continent with the removal of African orography (in *noAfOrog* as compared to control, and in *noGlOrog* as compared to *prAfOrog*). The major difference between *noAfOrog* and control simulations appears to be that the winds blowing into

DOI: 10.1002/joc

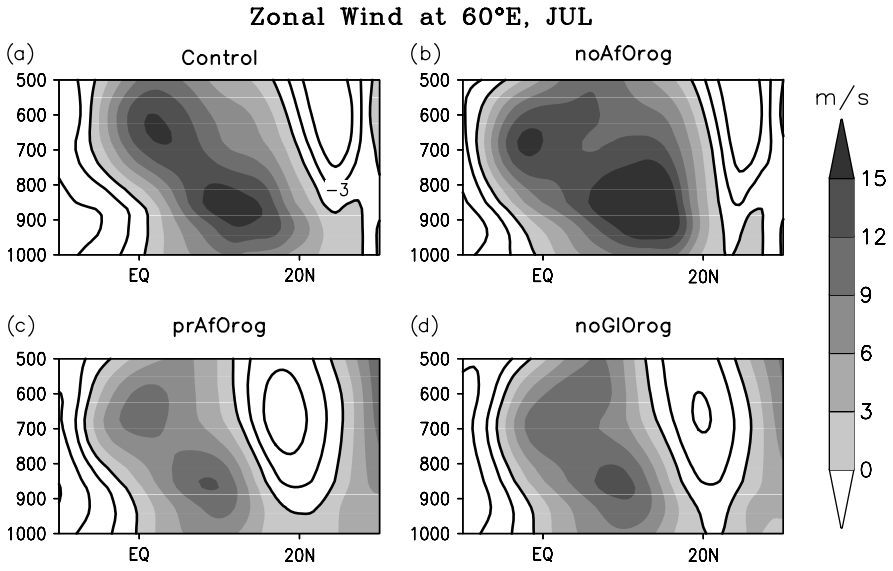

Figure 6. Zonal wind at 60 °E during July from (a) control (all orography present), (b) *noAfOrog* (all but African orography present), (c) *prAfOrog* (all but African orography absent), and (d) *noGlOrog* simulations (all orography absent).

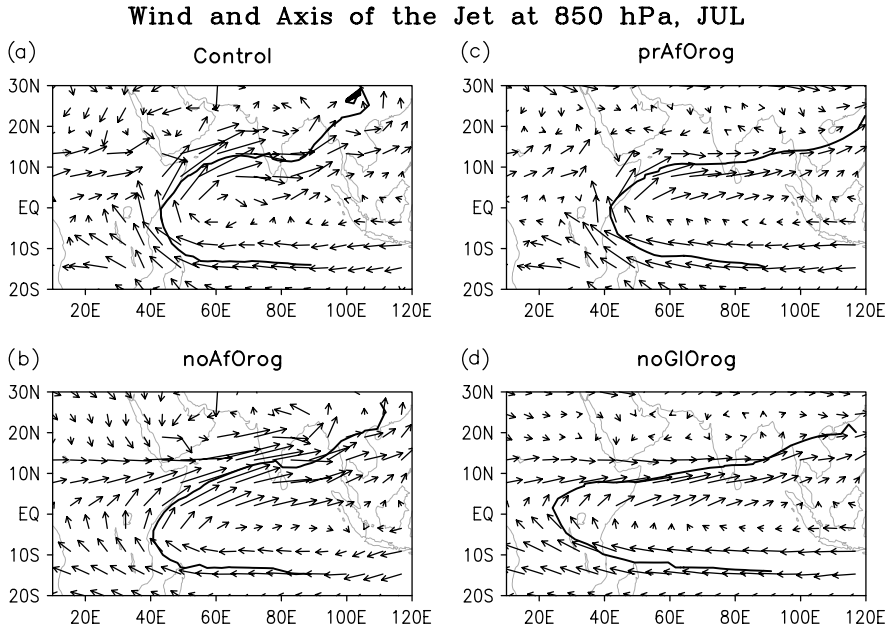

Figure 7. Vector wind at 850 hPa and the axis of the LLJ (dotted line) during July from (a) control, (b) *noAfOrog*, (c) *prAfOrog*, and (d) *noGlOrog* simulations.

the Indian sub-continent in the control (as in observations) are predominantly cross-equatorial with the flow concentrated near the African coast. The winds blowing across the African continent converge over the East African highlands. In the *noAfOrog* simulation, the convergence over the East African highlands (which have been removed) is reduced, and the zonal flow from the African continent (in addition to the cross-equatorial flow) contributes significantly to the westerly jet over the Arabian Sea. The cross-equatorial winds in the *noAfOrog* simulation turn over a larger region in comparison to the control simulations where the cross-equatorial flow is concentrated over the Somali coast. It was also noticed in Chakraborty *et al*. (2006) that the date of the onset of the monsoon over the Indian region was delayed, and the seasonal mean precipitation was decreased in *prAfOrog* simulation as compared to *noGlOrog* simulation. This change was similar to that noticed between control and *noAfOrog* simulations, and it can be said that the reason behind increased precipitation without African mountains was due to zonal wind and moisture flux towards the Indian region from over the African continent.

We next examine whether the occurrence of the LLJ is related to presence of the African continent (i.e. presence of land–sea contrast as suggested by Krishnamurti *et al*. (1976)), or African orography (as suggested by Sashegyi and Geisler, 1987), or whether it occurs as a response to the monsoonal heat source. We study this by using

DOI: 10.1002/joc

an aqua-planet simulation with an off-equatorial SST maximum.

4.1. An aqua-planet simulation

We next study the circulation pattern in an aqua-planet simulation. To mimic the off-equatorial monsoonal heat source in the northern Bay of Bengal, we introduced a circular-shaped SST maximum (302 K) at 90 °E, 20 °N. The SST values go linearly down to 288 K, about 10° outside its center. The results are shown in Figure 8. We notice that the flow is qualitatively similar to control simulation (i.e. a cross-equatorial flow to the west of the SST maximum followed by a zonal jet). We find that the highest rainfall over the SST maximum is at 90 °E. We also find that the maximum meridional wind at the equator is at 30° west of the rainfall maximum. However, the magnitude of the meridional wind is much lower than observed. The occurrence of meridional wind maximum, which is about 30° west of the rainfall maximum, is a response of the flow to the monsoonal heating. The exact location of the jet is related to the strength of the off-equatorial heat source. This is consistent with the theory proposed by Matsuno (1966); Webster (1972) and Gill (1980), that diabatic heating in the Tropics can induce circulation. This heat source is generally 20–30° west of the off-equatorial heat source. Hence, the monsoonal heat source over the South Asian region can be attributed to the cross-equatorial flow along 40°–50 °E. The presence of Africa (which increases the land–sea contrast) and African orography intensifies the cross-equatorial flow. As seen in the simulations without African mountains, absence of East African highlands allows mass convergence from the African continent into the Indian monsoon region. Thus, the presence of African mountains prevents this zonal convergence and causes the flow to become more strongly cross-equatorial (thus increasing the magnitude of cross-equatorial winds). Interestingly, we also find stronger meridional winds in the *prAfOrog* simulation (i.e. where only the mountains over Africa are considered). We find that though the rainfall in this simulation is lower than even the 'no-global orography' simulation, and the onset is delayed by about 45 days vis-a-vis control, the strength of the cross-equatorial flow is higher than the simulation without African orography. The aqua-planet simulation has highlighted the role played by monsoon latent heating in controlling the location at which the jet crosses the Equator. We can see from Figure 5 that the monsoonal heat source extends up to 75 °E in all the simulations, and from Figure 7, the cross-equatorial flow is most prominent at 45 °E, i.e. about 30° west of the heat source. In the aqua-planet simulation also, the cross-equatorial jet is about 30° west of the heat source. The actual planet simulation, when compared with the aqua-planet simulations, clearly shows that the position of the cross-equatorial jet is related to the occurrence of monsoonal heat source over the Indian region. The East African highlands intensify this cross-equatorial jet.

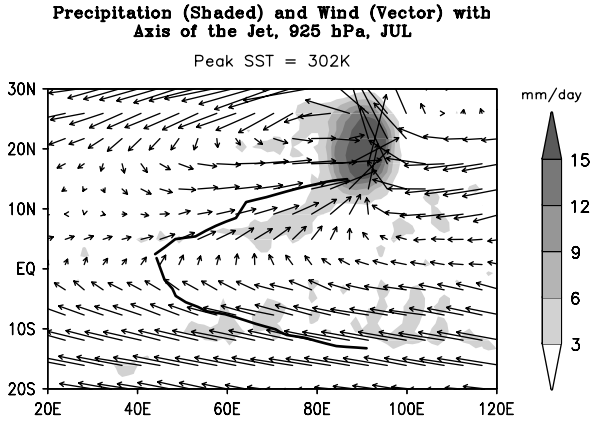

Figure 8. Vector wind at 925 hPa and precipitation (shaded) along with the axis of the LLJ during July from the aqua-planet simulation.

4.2. Strength of the jet and Indian monsoon rainfall

We have seen that there are two facets to the LLJ. One is the meridional jet near the Somali coast, and the other is the westerly (zonal) jet over the Indian monsoon region. We find that the strength of the meridional jet is not related to the strength of Indian monsoon rainfall but to the presence of the East African highlands. If the equatorial jet were to be related to the strength of the monsoonal heat source then the strength of the meridional jet should have been much higher in the 'no-African mountains' simulation than in the control simulation. We try to understand this behaviour of the cross-equatorial meridional jet. The off-equatorial monsoonal heat source creates pressure gradients in the meridional direction. This leads to a predominantly zonal flow (due to geostrophy) with a secondary cross-equatorial flow feeding into this zonal flow. The presence of the East African mountains prevents the zonal flow in the lower troposphere beyond the African coast. The conservation of mass would require a higher proportion of flow to be meridional at this longitude. This in turn amplifies the cross-equatorial jet. However, the magnitude of the westerly jet over the Arabian Sea is strongly linked to the strength of the Indian monsoon rainfall. Strongest winds during July are found in the 'no-Africa' simulation, which has the highest rainfall and weakest winds in the 'no-global' simulation which has the lowest rainfall. Figure 9 (a, b) show the relationship between the strengths of the Indian summer monsoon precipitation and low-level zonal wind over the western Arabian Sea from the model simulations. The area of average for precipitation was 70°–100 °E, 10°–20 °N, and that for zonal wind at 850 hPa level was 55°–60 °E, 5°–10 °N. All the 4 months of the summer season (June–September) have been shown separately for each of the following experiments controls, *noGlOrog* and *noAfOrog*. Figure 9b shows that, in general, as the precipitation increases over the Indian region, the strength of the low-level zonal wind also increases over the western Arabian Sea. The linear correlation coefficient of these 12 points (4 months and 3 simulations) was 0.85. This was significant at 99% level while using a test on correlation coefficient for small numbers (Haan, 1995). This relationship between zonal

DOI: 10.1002/joc

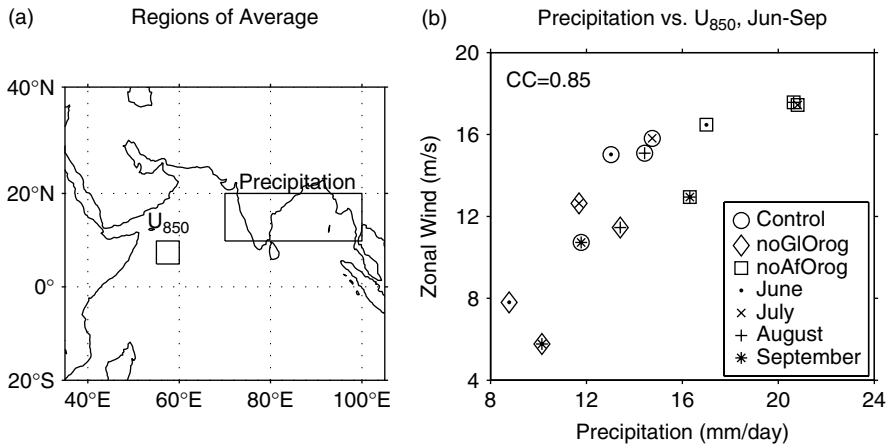

Figure 9. Relation between the strength of zonal wind at 850 hPa over the western Arabian Sea near the Somalia coast, and precipitation over the Indian region. (a) Regions of average for zonal wind (55°–60°E, 5°–10°N) and precipitation (70°–100°E, 10°–20°N). (b) Precipitation and zonal wind averaged over the regions shown in panel (a) during June–September from control, *noGlOrog* and *noAfOrog* simulations. Linear correlation coefficient between these 12 points is indicated at the top of the panel. This correlation coefficient is significant at 99% level.

wind over the western Arabian Sea and precipitation over the Indian region is consistent with the observation that the strength of the zonal wind over the Somalia coast lags by about 3 days in relation to the strength of precipitation over the Bay of Bengal (Chakraborty *et al*., 2002).

5. Conclusions

We have studied the LLJ in observations and with an AGCM. The role of orography over the entire world as well as over the African region alone was studied. It was seen that upon removal of African orography, the strength of the Indian monsoon increased. The strength of the low-level westerly jet over the Arabian Sea also increased. Qualitatively, the structure of winds between the African coast and the Indian land mass remained the same but the magnitudes changed significantly. We find that the removal of African orography did not change the position of equatorial meridional wind maximum (around 45°E). In the 'no-Africa' simulation, the vertical structure of meridional wind however, is very different. The concentration of isotachs off the African coast is absent.

We also find that the strength of the meridional jet is not related to magnitude of the Indian monsoon rainfall though the occurrence of the Indian monsoon rainfall is necessary. The magnitude of the low-level westerly jet over the Arabian Sea is directly linked to the strength of the Indian monsoon rainfall.

From the aqua-planet simulation with an off-equatorial heat source (to mimic the position of rainfall away from the Equator during the Indian monsoon season) we find that the longitudinal location of the strongest meridional winds occur about 30° west of the monsoonal heat source. The occurrence of the highest meridional winds near the East African coast is on account of the combination of the western boundary current (due to the presence of the African mountains) driven by an off-equatorial heat source. In the absence of these mountains, air from Africa converges over the Indian monsoon region and the cross-equatorial flow weakens.

The analysis presented above is based on a GCM simulation with prescribed SST for the year 1998. We had conducted some simulations for the year 1997, and also with the Kuo convection scheme (Anthes, 1977). The results were essentially similar. However, it is well known that the Indian monsoon influences the conditions of the ocean and is, in turn, influenced by conditions of the surrounding oceans. The impact of African orography on the Arabian Sea will be examined sometime later.

References

Anthes RA. 1977. A cumulus parameterization scheme utilizing a one-dimensional cloud model. *Monthly Weather Review* **105**: 270–286.

Chakraborty A, Nanjundiah RS, Srinivasan J. 2002. Role of Asian and African orography on Indian summer monsoon. *Geophysical Research Letters* **29**:, DOI: 10.1029/2002GL015522.

Chakraborty A, Nanjundiah RS, Srinivasan J. 2006. A theory for the onset of Indian summer monsoon from perturbed orography simulations in a GCM. *Annales De Geophysique* **24**: 2075–2089.

Fels SB, Schwarzkopf D. 1981. An efficient, accurate algorithm for calculating CO_2 15 μm band cooling rates. *Journal of Geophysical Research* **86**(C2): 1205–1232.

Findlater J. 1969a. Inter-hemispheric transport of air in the lower troposphere over the western Indian Ocean. *Quarterly Journal of the Royal Meteorological Society* **95**: 400–403.

Findlater J. 1969b. A major low level current near the Indian ocean during northern summer. *Quarterly Journal of the Royal Meteorological Society* **95**: 362–380.

Gill AE. 1980. Some simple solutions for heat induced tropical circulation. *Quarterly Journal of the Royal Meteorological Society* **106**: 447–462.

Grell GA. 1993. Prognostic evaluation of assumptions used by cumulus parameterization. *Monthly Weather Review* **121**: 764–787.

Haan CT. 1995. *Statistical Methods in Hydrology*, 1st edn. Affiliated East-West Press: New Delhi, India.

Hoskins B, Rodwell M. 1995. A model of the Asian summer monsoon, Part-I: the global scale. *Journal of Climate* **8**: 1–12.

Joseph PV, Raman PL. 1966. Existence of low level westerly jet-stream over peninsular India during July. *Indian Journal of Meteorology and Geophysics* **17**: 437–471.

Joseph P, Sijikumar S. 2004. Intraseasonal variability of the low-level jet stream of the Asian summer monsoon. *Journal of Climate* **17**: 1449–1458.

Kitoh A. 2004. Effects of mountain uplift on East Asian summer climate investigated by a coupled atmosphere-ocean GCM. *Journal of Climate* **17**: 783–802.

Krishnamurti TN, Wong V. 1979. A simulation of cross equatorial low over Arabian Sea. *Journal of the Atmospheric Sciences* **36**: 1895–1907.

Krishnamurti TN, Molinari J, Pan HL. 1976. Numerical simulation of the Somali Jet. *Journal of the Atmospheric Sciences* **33**: 2350–2362.

Krishnamurti TN, Wong V, Pan HL, Pasch R, Molinari J, Ardanuy PA. 1983. Three dimensional planetary boundary layer model for Somali Jet. *Journal of the Atmospheric Sciences* **40**: 894–908.

Lacis AA, Hansen JK. 1974. A parameterization for the absorption of solar radiation in the earth's atmosphere. *Journal of the Atmospheric Sciences* **32**: 118–133.

Matsuno T. 1966. Quasi-geostropic motions in the equatorial area. *Journal of the Meteorological Society of Japan* **44**: 25–43.

Mawson MH, Cullen MJP. 1992. An idealized simulation of the Indian monsoon using primitive-equation and quasi-equilibrium models. *Quarterly Journal of the Royal Meteorological Society* **118**: 153–164.

Pan HL, Mahrt L. 1986. Interaction between soil hydrology and boundary layer development. *Boundary-Layer Meteorology* **38**: 185–202.

Park S, Hong S-Y. 2004. The role of surface boundary forcing over south Asia in the Indian summer monsoon circulation: a regional climate model sensitivity study. *Geophysical Research Letters* **31**: L12112, DOI:10.1029/2004GL019729.

Reynolds RW, Smith TM. 1994. Improved global sea surface temperature analyses using optimum interpolation. *Journal of Climate* **7**: 929–948.

Rodwell M, Hoskins B. 1995. A model of the Asian summer monsoon, Part II: Cross-equatorial flow and PV behavior. *Journal of the Atmospheric Sciences* **53**: 1341–1356.

Sashegyi KD, Geisler JE. 1987. A linear model study of the cross-equatorial flow forced by summer monsoon heat sources. *Journal of the Atmospheric Sciences* **44**: 1706–1722.

Sela JG. 1982. The NMC spectral model. NOAA Technical Report, NWS-30. NOAA: USA; 36.

Sela JG. 1988. The new NMC operational spectral model. Eighth conference on numerical weather prediction. February 22–26, Baltimore.

Slingo J, Spencer H, Hoskins B, Berrisford P, Black E. 2005. The meteorology of the Western Indian Ocean, and the influence of the East African Highlands. *Philosophical Transactions of the Royal Society A* **363**: 25–42.

Srinivasan J, Nanjundiah RS. 2002. The evolution of Indian summer monsoon in 1997 and 1983. *Meteorology and Atmospheric Physics* **79**: 243–257.

Uppala SM, Kallberg PW, Simmons AJ, Andrae U, Bechtold VD, Fiorino M, Gibson JK, Haseler J, Hernandez A, Kelly GA, Li X, Onogi K, Saarinen S, Sokka N, Allan RP, Andersson E, Arpe K, Balmaseda MA, Beljaars ACM, Van De Berg L, Bidlot J, Bormann N, Caires S, Chevallier F, Dethof A, Dragosavac M, Fisher M, Fuentes M, Hagemann S, Holm E, Hoskins BJ, Isaksen L, Janssen PAEM, Jenne R, McNally AP, Mahfouf JF, Morcrette JJ, Rayner NA, Saunders RW, Simon P, Sterl A, Trenberth KE, Untch A, Vasiljevic D, Viterbo P, Woollen J. 2005. The ERA-40 re-analysis. *Quarterly Journal of the Royal Meteorological Society* **131**: 2961–3012.

Webster P. 1972. Response of the tropical atmosphere to local, steady forcing. *Monthly Weather Review* **100**: 517–540.

DOI: 10.1002/joc